Published in Journal of Electroanalytical Chemistry 2002, vol 526, p 10-18
DOI: 10.1016/S0022-0728(02)00745-3

Evaluation of the Koutecký-Koryta approximation for voltammetric currents generated by metal complex systems with various labilities

Herman P. van Leeuwen*[a+], Jaume Puy[b], Josep Galceran[b] and Joan Cecília[c]

[a]*Laboratory of Physical Chemistry and Colloid Science, Wageningen University, Dreijenplein 6, 6703 HB Wageningen, The Netherlands.*

[b]*Departament de Química,* [c]*Departament de Matemàtica, Universitat de Lleida, Rovira Roure 177, 25198, Lleida, Spain*

* Corresponding author. e-mail address: herman@fenk.wau.nl

+ Iberdrola professor at Barcelona & Lleida Universities, Spain, February-July 2000.

Abstract

The voltammetric response of metal complex systems with various labilities is analyzed by rigorous numerical simulation with the Finite Element Method of the time-dependent concentration profiles of the different species. The ensuing exact fluxes and the corresponding currents are compared to those derived from the Koutecky-Koryta (KK) approximation which assumes a discontinuous transition in the concentration profiles from non-labile to labile behavior. The results indicate a relatively far-reaching correctness of the KK approximation in the complete kinetic range from non-labile to labile complexes, as long as the kinetic flux is computed from the effective concentration of the complex in the reaction layer. Some approximate analytical expressions for this concentration are provided. The KK approximation is shown to be applicable for any metal-to-ligand ratio, provided that the thickness of the reaction layer is expressed in terms of the ligand concentration at the electrode surface.

Keywords:

Homogeneous complexation; Finite Element Method; Reaction layer; Lability; Planar electrode; Concentration profiles

Introduction

Over the nineties there has been a substantial growth of interest in *dynamic metal speciation*, which not only covers the equilibrium distribution of the different metal species but also the kinetic characteristics of their interconversion [1-3]. Kinetically defined categories of behavior of metal complexes range from inert to dynamic, the latter comprising various degrees of lability. The different notions have been defined on the basis of the voltammetric response of systems with electroinactive complex species and electroactive uncomplexed hydrated metal ions [4-7].

The case of *inert* complexes is rather trivial because such complexes do not contribute at all to the metal ion reduction process. The voltammetric response is then identical to that of the mere free metal ion. The distinction between labile and non-labile complexes is much more subtle since both of them refer to systems with relatively high rates of conversion of complex species into free metal ions. *Labile* complexes are characterized by such high rates of dissociation/re-association that, on any relevant spatial scale, full equilibrium between complexed and free metal is maintained. Consequently, interfacial processes involving the free metal (e. g. electrochemical reduction) are then limited by coupled diffusion of complex and free metal. *Non-labile* complexes represent the other extreme within the dynamic range where the effective rate of dissociation is much lower than that of the diffusive supply. In that case, the rate of dissociation (a volume reaction) determines the contribution of the complex to the interfacial metal ion flux.

The distinction between labile, non-labile and inert complexes is of great importance in the practice of metal speciation [1,8]. For a given total metal concentration, the interfacial fluxes for the three types of complexes may differ drastically. The intermediate case of partially labile (quasi-labile) complexes [4] is rather involved because of the simultaneous significance of the association /dissociation rates of the volume complexation reaction and the diffusional terms in the leading conservation equations. The problem was already tackled by Brdička, Koutecký and other members of the Czechoslovak School [9-14] and this resulted in a rather comprehensive analysis of the so-called kinetic currents. Within this frame, Koutecký and Koryta [14-16] came up with an apparently useful approximation, based on the *spatial separation of the depletion layer into non-labile and labile regimes*. The borderline between the two regimes would be located at the boundary of the reaction layer, situated at a distance $x = \mu$ from the surface. For x smaller than μ, i. e. within the reaction layer, the contribution from the complex is considered to be purely kinetic, whereas for $x > \mu$, the kinetics are supposed to be infinitely fast and the complex contributes merely via the coupled diffusion with free metal. This discontinuous approach, which we shall denote as the Koutecký-Koryta (KK) approximation, is extremely simple and might provide a practically attractive method for dealing with the partially-labile regime.

This paper aims at a rigorous analysis of the partially-labile situation via numerical simulation of the concentration profiles of the different metal species under various kinetic conditions (see Appendix for computational details on the numerical procedure). This will enable us to deduce the exact fluxes of the different species at any point in space and time which can then be compared to the fluxes derived from the KK approach. The results precisely define the range of validity of the KK approximation.

General

We consider the common case of an electroactive metal ion M (reducible to M^0) in the presence of a ligand L with which it may form the electroinactive complex ML

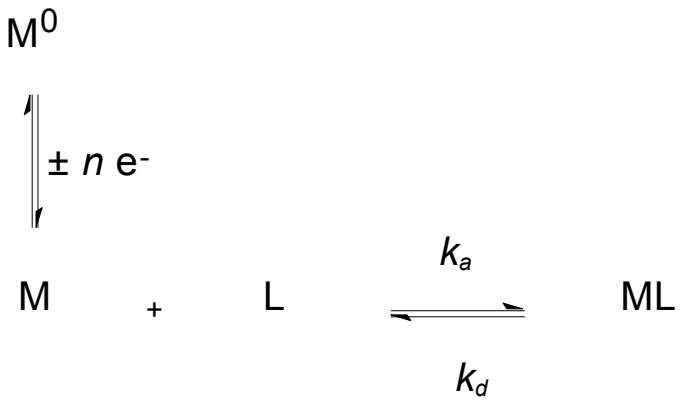

(1)

The quotient k_a/k_d of the rate constants defines the stability constant *K* of the complex. The ratio *Q* is defined as

$$Q = \frac{c_{\mathrm{ML}}}{c_{\mathrm{M}} c_{\mathrm{L}}} \tag{2}$$

which equals *K* if equilibrium (1) is attained.

If diffusion towards a stationary planar electrode is the sole transport mechanism, the conservation equations for M, ML and L read

$$\frac{\partial c_i(x,t)}{\partial t} = D_i \frac{\partial^2 c_i(x,t)}{\partial x^2} \pm k_d \left(c_{\mathrm{ML}} - K c_{\mathrm{M}} c_{\mathrm{L}} \right) \tag{3}$$

with the plus sign for *i*=M or L and the minus sign for *i*=ML.

The usual initial and boundary conditions are

$$t = 0, x \geq 0 \qquad \frac{c_{\mathrm{ML}}}{c_{\mathrm{M}}\ c_{\mathrm{L}}} = \frac{c^*_{\mathrm{ML}}}{c^*_{\mathrm{M}}\ c^*_{\mathrm{L}}} \tag{4a}$$

$$t > 0, \quad x \to \infty \qquad c_i = c_i^* \quad i = \mathrm{M, L, ML} \tag{4b}$$

where *t* is time, *x* the distance from the electrode surface and c_i^* the bulk concentration of *i*.

In case of a sufficiently large excess of ligand L the association reaction is pseudo first-order and we define

$$K\, c_{\mathrm{L}}^* = K' = \frac{c_{\mathrm{ML}}^*}{c_{\mathrm{M}}^*} \tag{5a}$$

$$k_a\, c_{\mathrm{L}}^* = k_a' \tag{5b}$$

Chronoamperometric limiting current conditions are defined by

$$t \geq 0,\, x = 0 \quad \begin{cases} c_{\mathrm{M}} = 0 \\ \partial c_{\mathrm{ML}} / \partial x = 0 \end{cases} \qquad \text{LimitingCurrent(6)}$$

which completes the formulation of the problem.

Complex systems are divided into static (or inert) and dynamic categories. The distinction is based on the values of the effective chemical rate constants k_d and k_a', relative to the effective time scale *t*. According to the official definitions [6], and in full agreement with the restrictions of the classical treatments [14], both non-labile and labile complex systems are subject to the condition

$$k_d t \quad , \quad k_a' t \quad >> 1 \tag{7}$$

The physical meaning is that the conversion of M into ML and vice versa is fast on the time scale considered, and the corresponding regime has been denoted as 'dynamic' [5]. It is important to bear in mind that fulfillment of condition (7) does not imply that

equilibrium (1) is maintained on every relevant spatial scale contained in an experiment on time-scale *t*. The condition is concerned with the *volume* complexation reaction (1) and its fulfillment does not warrant the maintenance of equilibrium in an interfacial process of consumption of free metal ions. This feature actually forms the heart of the mere existence of the so-called reaction layer where the dissociation of ML is not fast enough to 'follow' the depletion of M. The reaction layer is defined by its thickness μ [7,10,17,18]

$$\mu = \left(D_{\mathrm{M}} / k_a^{'}\right)^{1/2} = \left(D_{\mathrm{M}} / \left(k_a c_{\mathrm{L}}^{*}\right)\right)^{1/2} \tag{8}$$

Concentration profiles and fluxes of M and ML

A. The non-labile regime

By various definitions, non-lability is related to the rate of dissociation of the complex being so slow that depletion of ML is negligible even in the immediate vicinity of the electrode surface. Thus it is characterized by the combination of the conditions (7) and

$$c_{\mathrm{ML}}^{\phi} / c_{\mathrm{ML}}^{*} \approx 1 \tag{9}$$

where c_{ML}^{ϕ} denotes concentration in the reaction layer.

The flux of free metal, generated in the reaction layer adjacent to the electrode surface is then simply given by

$$J_{kin} = k_d \; c_{\mathrm{ML}}^{*} \; \mu \tag{10}$$

Typical concentration profiles of M and ML in the non-labile regime are given by Fig. 1. Needless to add that *Q/K* significantly deviates from 1 only for $x < \mu$.

In case of a sufficient excess of ML over M ($c^*_{T,L} > c^*_{T,M}$, $K' >> 1$, $c^*_{T,L}$ and $c^*_{T,M}$ labelling the total ligand and total metal bulk concentrations respectively), the complex is able to maintain an approximately constant c_M ($c_M \approx c^*_M$) from the bulk down to $x \approx \mu$. The limitations of the free metal ion "buffering capacity" of ML only shows up at distances less than μ where the diffusive depletion of M is faster than the replenishing by dissociation of ML. The non-labile regime, characterized by Fig. 1, is the limiting case where the flux of M is governed by the dissociation of ML in the reaction layer. Since, unlike the diffusion layer thickness $\delta_M \equiv \sqrt{\pi D_M t}$, μ is not a function of time, the apparent steady state flux may be formulated as diffusional flux of M *within the reaction layer*:

$$J_M = D_M c^*_M / \mu = k_d \, c^*_{ML} \, \mu \qquad (11)$$

which is immediately verified using (5) and the definition of μ, eqn. (8).

Conceptually, the non-labile regime is of a special nature: on the one hand it requires high rate constants k_d and k_a' to fulfill condition (7) so that $\mu << \delta_M$, and on the other hand k_d must be so low that depletion of ML inside the reaction layer with thickness μ is not appreciable. It is this potentially conflicting set of requirements that has given rise to the differentiated definition of the notion of lability [19,20].

B. The labile regime

Labile systems obey condition (7), and have such high k_d values that depletion of ML is practically complete. Thus they are characterized by kinetic fluxes that largely outweigh the diffusive fluxes J_{dif} :

$$J_{kin}/J_{dif}\left(=k_d\ c^*_{\mathrm{ML}}\ \mu\Big/\frac{D_{\mathrm{ML}}\ c^*_{\mathrm{ML}}}{\left(\pi D_{\mathrm{ML}}t\right)^{1/2}}\right)>>1 \qquad (12)$$

This condition has been discussed at length in the literature [21]. The corresponding typical profiles of M and ML are given by fig. 2. In agreement with the fulfillment of condition (7), meaning that $\mu << \delta$, the labile situation is characterized by $c^0_{\mathrm{ML}}/c^*_{\mathrm{ML}} \to 0$, where superscript zero indicates the volume concentration at $x = 0$. Equilibrium between M and ML is essentially maintained to such an extent that the overall metal flux at the surface is given by the coupled diffusion of M and ML. Thus, if their diffusion coefficients are different, the flux is proportional to the weighted mean diffusion coefficient ($\overline{D} \equiv \frac{c^*_{\mathrm{M}}}{c^*_{\mathrm{T,M}}} D_{\mathrm{M}} + \frac{c^*_{\mathrm{ML}}}{c^*_{\mathrm{T,M}}} D_{\mathrm{ML}}$) and the total concentration of the free and labile metal species [22].

C. The partially-labile regime

The transition between labile and non-labile regimes is characterized by intermediate values of $c^0_{\mathrm{ML}}/c^*_{\mathrm{ML}}$ which corresponds to J_{kin}/J_{dif} being of order unity

$$J_{kin}/J_{dif} \approx 1 \qquad (13)$$

The simulation reveals that approaching the electrode from the bulk solution, there is a certain region with depletion of M, together with a metal flux low enough to be "followed" by the complex so that equilibrium is maintained. This is the region where kinetics can be considered infinitely fast in the Koutecký-Koryta approximation. Closer to the electrode surface, the metal flux increases and for x less than μ, the rate of

dissociation of ML becomes limiting. The concentration of ML tends to an approximately constant, c_{ML}^{ϕ}, to reach the prescribed zero slope at the surface (see (6)). Fig. 3 illustrates this and the corresponding explosion of the disequilibration factor Q/K towards smaller x in the reaction layer region. The effective current is then due to the diffusion of the free metal arising from complex dissociation (the incoming flux of free metal to the reaction layer is negligible for sufficiently large K') and the kinetic flux approaches

$$J_{kin} = k_d \; c_{\mathrm{ML}}^{\phi} \; \mu \qquad (14)$$

by extension of the Koutecký-Koryta approximation to the partially-labile regime.

In order to check the results of this expression, Fig 4 plots (i) the current, as represented by the metal flux at the electrode surface $J_{\mathrm{M}}^{0} = D_{\mathrm{M}}\left(\frac{\partial c_{\mathrm{M}}}{\partial x}\right)_{x=0}$, (ii) the kinetic contribution to this flux, $J_{kin} = k_d \; c_{\mathrm{ML}}^{\phi} \; \mu$, (iii) the flux of complex arriving at the reaction layer, $J_{\mathrm{ML}}^{\mu} = D_{\mathrm{ML}}\left(\frac{\partial c_{\mathrm{ML}}}{\partial x}\right)_{x=\mu}$, and (iv) $c_{\mathrm{ML}}^{0} / c_{\mathrm{ML}}^{*}$, for increasing values of the dissociation rate constant. In the whole range of k_d values in the figure, the system is dynamic ($k_a' t, k_d t > 1$). The reaction layer thickness μ, as derived from k_a and c_{L}^{*}, is constant for all the points of the figure; this implies that the stability constant varies inversely with k_d.

For $k_d < 10^2\ \mathrm{s}^{-1}$, J_{M}^{0} is almost zero, since there is no noticeable dissociation and almost no free metal in bulk solution (we are in excess ligand conditions and $K' >> 1$). As k_d increases, the metal flux increases up to a plateau ($10^4\ \mathrm{s}^{-1} < k_d < 10^6\ \mathrm{s}^{-1}$) where the labile

regime is reached as is recognized in the figure since $c^0_{\mathrm{ML}}/c^*_{\mathrm{ML}} \to 0$. In this plateau, the current is sensitive only to the equilibrium speciation, being J^0_{M} proportional to $\bar{D}c^*_{\mathrm{T,M}}$. A further increase of k_d leads to a new increase in J^0_{M} since the equilibrium is shifted towards free metal as the stability constant $K = k_a/k_d$ decreases ($\varepsilon K'$ no longer larger compared to unity). For k_d high enough ($K' << 1$), a new plateau of J^0_{M} is reached corresponding to the simple case of only free metal being present.

It should be noticed that J_{kin}, defined as (14) in the extension of the Koutecký-Koryta approximation to the partially-labile regime, is a good approximation for J^0_{M} in all the k_d range up to the labile situation. This result deserves some comments:

i) a reaction layer with local disequilibration is present in all the cases, even under labile conditions. As it has been noticed, the condition of lability expressed in terms of bulk properties, eqn. (12), does not imply fulfillment of local equilibrium at any spatial point and time. Actually, the diffusive flux of the metal increases approaching the electrode while J_{kin} decreases since it depends not only on k_d but also on the local concentration c^{ϕ}_{ML}. This last dependence evidences that under labile conditions, the inequality $J_{kin} > J_{dif}$ with J_{kin} defined for c^{ϕ}_{ML}, cannot be maintained for $x < \mu$ since J_{kin} and c^{ϕ}_{ML} tend to zero.

ii) Although J_{kin} as defined by (14) is a good approximation for J^0_{M}, there is no true steady state since $J_{kin} > J^{\mu}_{\mathrm{ML}}$. Due to this inequality, a time dependent c^{ϕ}_{ML} arises, and for fixed *t*, c^{ϕ}_{ML} decreases as k_d increases. Fig. 4 clearly shows that the decrease of $c^0_{\mathrm{ML}}/c^*_{\mathrm{ML}}$ towards zero is correlated with the disparity of J^{μ}_{ML} and J_{kin}.

Given the simplicity and accuracy of J_{kin} it is interesting to work out an approximate analytical expression for c_{ML}^{ϕ} in order to obtain a simple expression for the metal flux and for the current. Through the analytical resolution of the system (3-6) [23] under ligand excess conditions (flat profile for $c_{\mathrm{L}}(x,t)$), we can obtain c_{ML}^{0} which can be used as a good approximation for c_{ML}^{ϕ} :

$$c_{\mathrm{ML}}^{\phi} = \frac{c_{\mathrm{T,M}}^{*} D_{\mathrm{M}}}{\left(D_{\mathrm{M}} D_{\mathrm{ML}}\left(k_a^{'}+k_d\right)\right)^{3/2}}\left(D_{\mathrm{M}} k_d \sqrt{\frac{D_{\mathrm{M}} D_{\mathrm{ML}}}{k_a^{'}+k_d}}\left(k_a^{'}+k_d\right)+D_{\mathrm{ML}} k_a^{'}\sqrt{D_{\mathrm{M}} D_{\mathrm{ML}}\left(k_a^{'}+k_d\right)}\right) \mathrm{e}^{\frac{D_{\mathrm{M}} k_d^2\left(D_{\mathrm{ML}} k_a^{'}+D_{\mathrm{M}} k_d\right)^2 t}{D_{\mathrm{ML}}^3 k_a^{'2}\left(k_a^{'}+k_d\right)}} \mathrm{erfc}\left(\frac{D_{\mathrm{M}} k_d\left(D_{\mathrm{ML}} k_a^{'}+D_{\mathrm{M}} k_d\right)\sqrt{t}}{D_{\mathrm{ML}} k_a^{'}\sqrt{D_{\mathrm{M}} D_{\mathrm{ML}}\left(k_a^{'}+k_d\right)}}\right) \quad (15)$$

which, for large values of the argument of erfc (e. g. high k_d-values), can be approximated by

$$c_{\mathrm{ML}}^{\phi} = \frac{c_{\mathrm{T,M}}^{*} k_a^{'}}{k_d\sqrt{\pi\left(k_a^{'}+k_d\right)t}}\sqrt{\frac{D_{\mathrm{ML}}}{D_{\mathrm{M}}}} \quad \text{Per60.14 (16)}$$

whereas for small values of the argument of erfc (e. g. low k_d-values), (15) reduces to

$$c_{\mathrm{ML}}^{\phi} = \frac{c_{\mathrm{T,M}}^{*}\left(D_{\mathrm{ML}} k_a^{'}+D_{\mathrm{M}} k_d\right)}{D_{\mathrm{ML}}\left(k_a^{'}+k_d\right)}\left(1-\frac{2k_d\left(D_{\mathrm{ML}} k_a^{'}+D_{\mathrm{M}} k_d\right)}{D_{\mathrm{ML}} k_a^{'}}\sqrt{\frac{D_{\mathrm{M}} t}{\pi D_{\mathrm{ML}}\left(k_a^{'}+k_d\right)}}\right) \quad \text{Per60.14 (17)}$$

Expressions (16) and (17) are plotted in dotted lines in fig. 4 showing a good agreement with c_{ML}^{ϕ} in both limiting kinetic regimes, but both of them differing from the exact results at intermediate values of c_{ML}^{ϕ} .

D. The Koutecký-Koryta approximation for a quasi-labile system with any ligand to metal ratio

This section examines the applicability of the Koutecký-Koryta approximation under non-excess ligand conditions. Fig. 5 is analogous to Fig. 4 but for a system with total

metal concentration exceeding that of the total ligand concentration. At the lowest k_d-values, J_{M}^0 starts with a non zero constant value which reflects the flux of the exceeding free metal in bulk solution. As there is no significant dissociation of complex, the behavior of the system approaches that of an inert system with a metal profile extending up to $x = \delta_{\mathrm{M}}$ (see fig. 6). Increasing k_d, J_{M}^0 increases due to the contribution of the complex dissociation, but now, as Fig. 5 shows, J_{kin} is not a good approximation for the kinetic contribution to J_{M}^0. In order to elucidate this, normalized profiles of the species for $k_d = 5 \cdot 10^2$ s^{-1} are displayed in Fig. 7 (notice the logarithmic scale in abscissas). Basically, the metal concentration coincides with that of Fig. 6 with a concentration profile extending up to δ_{M}. Due to the high value of the stability constant involved with this k_d-value ($K = k_a / k_d = 2 \cdot 10^5\ \mathrm{mol}^{-1}\ \mathrm{m}^3$) the depletion of the metal does not appreciably affect the profile of the complex. In fact this case is similar to that of an infinite stability constant for which the ligand concentration is zero in bulk conditions, metal and complex becoming unrestricted with respect to the equilibrium condition [24].

Close to the electrode (for x decreasing below 10^{-5} m, in Fig. 7), the ligand concentration starts to increase. This forces c_{M} to approach zero in order to fulfil the equilibrium condition, as the value of Q/K close to unity indicates. Clearly, this is not a kinetic effect but an equilibrium one. Due to the high value of the stability constant involved, the increase of c_{L} takes place when the local total metal profile falls below the local total ligand concentration. This condition is fulfilled for x less than the position of the intersection of the metal and ligand concentration profiles. Below this distance, all the metal tends to be complexed due to the high value of the stability constant

involved. The profile of the complex is then that of the total metal concentration, and, as the total ligand concentration is constant, a decrease of c_{ML} implies a corresponding increase of c_{L}. The position of the intersection point and the pertaining concentrations (c_{M} and c_{L}) increases as k_d increases. The higher k_d, the more depleted the concentration profile of ML ($k_d \rightarrow \infty$ - labile conditions- the complex concentration starts from zero at the electrode surface) and the steeper the concentration profile of the ligand.

As can be seen in Fig 7, the position $x = \mu$ does not coincide with the boundary of the disequilibration layer which confirms that the kinetic contribution defined as $J_{kin} = k_d\, c_{\mathrm{ML}}^{\phi}\, \mu$ does not equal J_{M}^{0}. In fact this is expected since the life time of the free metal before reassociation depends on c_{L} and the c_{L}-value close to the electrode is far away from the bulk c_{L}-value. So, we should redefine μ using the c_{L}-value in the reaction layer, c_{L}^{ϕ}:

$$\mu^{\phi} = \left(D_{\mathrm{M}} \Big/ \left(k_a c_{\mathrm{L}}^{\phi} \right) \right)^{1/2} \tag{18}$$

which leads to quite a good agreement with the effective layer of disequilibration as can be seen in Fig. 7. Likewise, the kinetic contribution must also be redefined as

$$J_{kin} = k_d\, c_{\mathrm{ML}}^{\phi} \mu^{\phi} \tag{19}$$

J_{kin}, defined as (19), is also plotted in figure 5. It is a good approximation for J_{M}^{0} in the range where there is a non-negligible contribution of the dissociation to the metal flux. However, J_{kin} is not a good approximation for the kinetic contribution at low k_d-values when J_{M}^{0} tends to the inert value (as indicated in Fig. 5). In fact, this result is not

surprising since expression (19) has been suggested as direct extension of the kinetic contribution in the case with excess of ligand and $K' >> 1$. Under these conditions, J_{kin} equals the total flux and tends to zero for low k_d-values. This limiting value of J_{kin} does not apply for the non-excess ligand case since the metal flux tends to the inert flux. This free metal contribution is not included in (19) and is responsible for the disparity between J_{M}^{0} and J_{kin} defined as (19) for low k_d-values. On the other hand, excess ligand conditions hold close to the electrode surface for a k_d-value greater than 10^2 s^{-1} in fig. 5 (see also fig. 7) justifying the agreement between (19) and J_{M}^{0} in the kinetic range.

Finally it is interesting to examine the concentration profiles close to the electrode surface for a k_d-value corresponding to the non-labile range. Fig. 8 shows the concentration profiles of Fig. 6 magnified up to distances of the order of the reaction layer thickness. At distances of the order of μ^{ϕ}, the metal profile intersects with that of the ligand. However, the plateau of the profile of M observed for *x* below $x = 10^{-5}$ m in fig. 7, does not appear and μ^{ϕ} differs from the thickness of the effective disequilibration layer. In fact, the metal concentration profile is not affected by the intersection with the profile of the ligand, J_{M}^{0} being determined by δ_{M} and very different from J_{kin} (see Fig 5). The low c_{M} in the intersection point compared to that at a higher k_d, renders the shift of the complexation equilibrium ineffective. Hence the depletion plateau as observed in fig. 7 in the profile of c_{M} between $x = \mu^{\phi}$ and $x = 10^{-5}$ m does not occur.

In summary, as can be seen in fig. 5, when $c^*_{T,M} > c^*_{T,L}$, the Koutecky-Koryta approximation based on the spatial separation of a reaction layer and a labile layer can also be used with the corrections discussed in this section. J^0_M can be well approximated by J_{kin}, defined as (19), in the k_d range where $J_{kin} > D_M c^*_M / \delta_M$ whereas $D_M c^*_M / \delta_M$ is a good approximation for J^0_M in the remaining k_d range.

Conclusions

The Finite Element Method is suitable for the computation of the time-dependent concentration profiles of the different species in the voltammetric response of metal complex systems with various labilities. The obtained profiles can be analyzed in order to understand the behavior of the system. The corresponding fluxes are compared to the fluxes derived from the Koutecky-Koryta (KK) approximation which is based on a simplified infinitely sharp transition from non-labile to labile behavior at the boundary of the reaction layer. The comparison shows a relatively far-reaching correctness of the KK approximation in the complete kinetic range of complexes with varying labilities, as long as the kinetic flux is computed from the effective concentration of the complex in the reaction layer c^{ϕ}_{ML} (see eqn. (14)). This concentration is of great importance for the voltammetric response of the system and it can be defined by the approximate analytical expressions (16) and (17). The analysis confirms that close to the electrode surface there is a disequilibration layer (where $Q \neq K$) with a thickness of that of the reaction layer, even in the case of labile complexes.

The KK approximation (see eqn. (19)) is shown to be applicable for any metal-to-ligand ratio in the complex system, provided that the thickness of the reaction layer is expressed in terms of the local ligand concentration at the electrode surface (eqn. 18). In this case, however, the KK expression is a good approximation for the metal flux only

in the kinetic range under conditions where the contribution of the dissociation of the complex to the metal flux is significant.

Acknowledgements

The authors gratefully acknowledge support of this research by the Spanish Ministry of Education and Science (DGICYT: Project BQU2000-0642), and from the "Comissionat d'Universitats i Recerca de la Generalitat de Catalunya".

Appendix

Linear systems (i.e. excess of ligand) can be dealt with analytically [11,25,26], but non-linear homogeneous reaction-diffusion problems require numerical approaches [27] such as the Galerkin Finite Element Method (GFEM) [28-30]. Indeed, despite the domain is -in principle- infinite, the concentration profiles significantly differ from bulk values just in a small region close to the electrode. A few nodal points can be unevenly placed in this region so that high accuracy can be obtained in the GFEM solution of the spatial dependence of the problem with low computational cost.

We use the following transformations and simplifications:

1.- Nondimensional concentrations are defined as

$$\hat{c}_i \equiv c_i / c_i^* \qquad \text{XXX(A-1)}$$

2.- The space variable is re-scaled using the largest diffusion coefficient:

$$z \equiv x / \sqrt{D_{\mathrm{M}}} \qquad \text{XXX(A-2)}$$

3.- The differential equations are linearized by using the auxiliary variable

$$r(z,t) = k_d \left(c_{\mathrm{ML}}^* \hat{c}_{\mathrm{ML}}(z,t) - K \cdot c_{\mathrm{M}}^* \cdot \hat{c}_{\mathrm{M}}(z,t) \cdot c_{\mathrm{L}}^* \cdot \hat{c}_{\mathrm{L}}(z,t) \right) \qquad \text{XXX(A-3)}$$

4.- By solving a combination of the continuity equations (3) for L and ML with the equality of diffusion coefficients $D_{\mathrm{L}} = D_{\mathrm{ML}}$, we have

$$c_{\mathrm{L}} + c_{\mathrm{ML}} = c^{*}_{\mathrm{T,L}} \qquad \text{XXX(A-4)}$$

Then, eqns. (3)-(4) can be written as

$$\frac{\partial \hat{c}_{\mathrm{M}}}{\partial t} = \frac{\partial^2 \hat{c}_{\mathrm{M}}}{\partial z^2} + \frac{1}{c^{*}_{\mathrm{M}}}\, r \qquad \text{NormcM XXX(A-5)}$$

$$\frac{\partial \hat{c}_{\mathrm{L}}}{\partial t} = \varepsilon \frac{\partial^2 \hat{c}_{\mathrm{L}}}{\partial z^2} + \frac{1}{c^{*}_{\mathrm{L}}}\, r \qquad \text{NormcL XXX(A-6)}$$

$$r - k_{\mathrm{d}} \left(c^{*}_{\mathrm{T,L}} - c^{*}_{\mathrm{L}} \hat{c}_{\mathrm{L}} - K c^{*}_{\mathrm{M}} c^{*}_{\mathrm{L}} \hat{c}_{\mathrm{M}} \hat{c}_{\mathrm{L}} \right) = 0 \qquad \text{Kinetic XXX(A-7)}$$

where $\varepsilon \equiv D_{\mathrm{ML}} / D_{\mathrm{M}}$.

The initial condition is

$$\hat{c}_{\mathrm{M}}(z,0) = \hat{c}_{\mathrm{L}}(z,0) = 1 \qquad \text{XXX(A-8)}$$

The boundary conditions become:

$$\hat{c}_{\mathrm{M}}(\infty,t) = \hat{c}_{\mathrm{L}}(\infty,t) = 1, \quad \hat{c}_{\mathrm{M}}(0,t) = \left. \frac{\partial \hat{c}_{\mathrm{L}}}{\partial z} \right|_{z=0} = 0 \qquad \text{XXX(A-9)}$$

Linear piecewise interpolation functions have been used in the discretized weak formulation of the problem. Let $(z_1 = 0,\ z_2,\ \ldots\ ,\ z_N)$ be the vector of spatial grid points, with z_N large enough so that the differences between local and bulk concentrations are negligible. Using

$$\vec{c}_i(t) = \left(\hat{c}_i(z_1,t), \ldots, \hat{c}_i(z_N,t)\right), \; i = \mathrm{M,L} \qquad \text{XXX(A-10)}$$

$$\vec{r}(t) \; = \; \left(r(z_1,t), \; \ldots \; , \; r(z_N,t)\right), \qquad \text{XXX(A-11)}$$

$$p(t) = \left.\frac{\partial \hat{c}_M}{\partial z}\right|_{z=0} \qquad \text{XXX(A-12)}$$

one can write XXX(A-5) and XXX(A-6) as a system of ordinary differential equations in the time variable:

$$A \cdot \vec{c}\,'_{\mathrm{M}}(t) + B \cdot \vec{c}_{\mathrm{M}}(t) + \begin{pmatrix} p(t) \\ 0 \\ \vdots \\ 0 \end{pmatrix} - \frac{1}{c^*_{\mathrm{M}}} A \cdot \vec{r}(t) = 0 \qquad \text{MatrixcM XXX(A-13)}$$

$$A \cdot \vec{c}\,'_{\mathrm{L}}(t) + \varepsilon \cdot B \cdot \vec{c}_{\mathrm{L}}(t) - \frac{1}{c^*_{\mathrm{L}}} A \cdot \vec{r}(t) = 0 \qquad \text{MatrixcL XXX(A-14)}$$

where *A* and *B* are

$$A = \begin{pmatrix} \frac{h_1}{3} & \frac{h_1}{6} & 0 & \cdots & 0 & 0 \\ \frac{h_1}{6} & \frac{h_1+h_2}{3} & \frac{h_2}{6} & \cdots & 0 & 0 \\ 0 & \frac{h_2}{6} & \frac{h_2+h_3}{3} & \cdots & 0 & 0 \\ \vdots & \vdots & \vdots & \ddots & \vdots & \vdots \\ 0 & 0 & 0 & \cdots & \frac{h_{N-2}+h_{N-1}}{3} & \frac{h_{N-1}}{6} \\ 0 & 0 & 0 & \cdots & \frac{h_{N-1}}{6} & \frac{h_{N-1}+h_N}{3} \end{pmatrix} \qquad \text{XXX(A-15)}$$

$$B=\begin{pmatrix} \frac{1}{h_1} & -\frac{1}{h_1} & 0 & \cdots & 0 & 0 \\ -\frac{1}{h_1} & \frac{1}{h_1}+\frac{1}{h_2} & -\frac{1}{h_2} & \cdots & 0 & 0 \\ 0 & \frac{1}{h_2} & \frac{1}{h_2}+\frac{1}{h_3} & \cdots & 0 & 0 \\ \vdots & \vdots & \vdots & \ddots & \vdots & \vdots \\ 0 & 0 & 0 & \cdots & \frac{1}{h_{N-2}}+\frac{1}{h_{N-1}} & -\frac{1}{h_{N-1}} \\ 0 & 0 & 0 & \cdots & -\frac{1}{h_{N-1}} & \frac{1}{h_{N-1}}+\frac{1}{h_N} \end{pmatrix} \qquad \text{XXX(A-16)}$$

with $h_i = z_{i+1} - z_i$.

The Inverse-Euler Finite Difference method (to ensure stability of the calculations and avoid spurious oscillation of the solution) is applied to the resulting system (eqn. XXX(A-7), XXX(A-13) and XXX(A-14)), thus transforming the original coupled set of ordinary differential equations into a non linear algebraic system:

$$\left(\frac{1}{\Delta t}A + B\right)\cdot \vec{c}_{\mathrm{M}}(t+\Delta t) + \begin{pmatrix} p(t+\Delta t) \\ 0 \\ \vdots \\ 0 \end{pmatrix} - \frac{1}{c_{\mathrm{M}}^*}A\cdot\vec{r}(t+\Delta t) - \frac{1}{\Delta t}A\vec{c}_{\mathrm{M}}(t) = 0 \quad \text{XXX(A-17)}$$

$$\left(\frac{1}{\Delta t}A + \varepsilon B\right)\cdot \vec{c}_{\mathrm{L}}(t+\Delta t) - \frac{1}{c_{\mathrm{L}}^*}A\cdot\vec{r}(t+\Delta t) - \frac{1}{\Delta t}A\vec{c}_{\mathrm{L}}(t) = 0 \qquad \text{XXX(A-18)}$$

$$r_i(t+\Delta t) - k_d\left(c_{\mathrm{T,L}}^* - c_{\mathrm{L}}^*\hat{c}_{\mathrm{L}}(z_i,t+\Delta t) + Kc_{\mathrm{M}}^*c_{\mathrm{L}}^*\hat{c}_{\mathrm{M}}(z_i,t+\Delta t)\hat{c}_L(z_i,t+\Delta t)\right) = 0 \qquad \text{XXX(A-19)}$$
$$i = 1..N$$

with $\hat{c}_{\mathrm{M}}(z_1,t+\Delta t) = 0$, due to the boundary condition (6). This system is iteratively solved with a Newton-like method, modified in order to avoid loss of convergence [31].

One of the main advantages of the GFEM method is the use of arbitrary unequal spatial grids. In this case, a spatial grid with *ca.* 50 nodes has been used. The distances (in units of *z*) between nodes increase going from the electrode surface to the bulk solution (at some 10 units). The typical distances taken are: 10^{-5} units (8 nodes), $2\cdot10^{-5}$ units (4 nodes), $8\cdot10^{-5}$ units (1 node) and then the distances double until they reach around 10^{-1} units.

Values of the concentrations at each spatial position and time *t* are used as a first trial in the iterative solution of the algebraic resulting system at the next time interval, $t+\Delta t$. The time interval used is $\Delta t = 10^{-4}$ s.

FIGURES:

fig 1

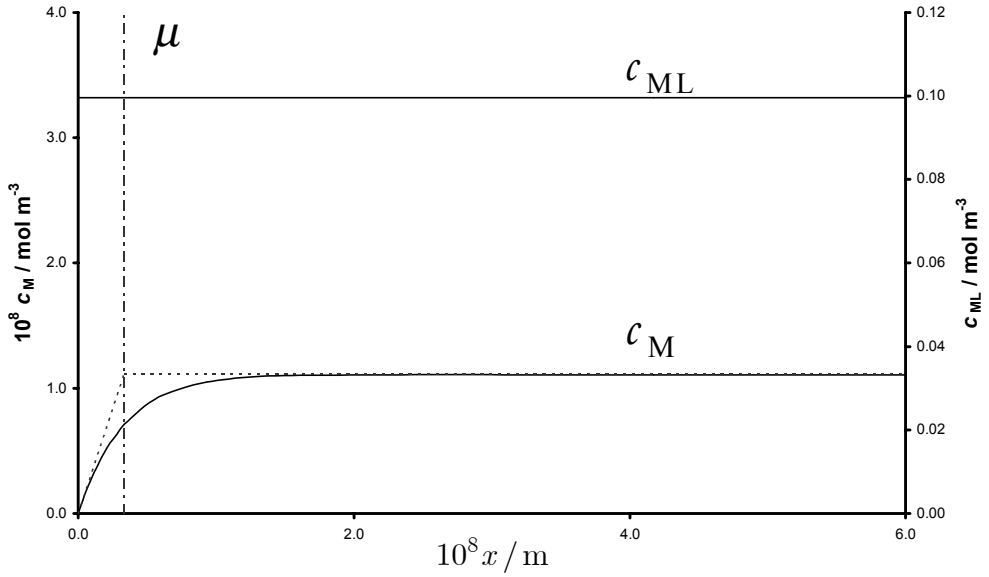

Fig 1: Concentration profiles of c_M (referred to the left ordinate axis) and c_{ML} (referred to the right ordinate axis) for a non-labile case. Parameters: $c^*_{T,L}$ = 1 mol m^{-3}, $c^*_{T,M}$ = 0.1 mol m^{-3}; k_a = 10^8 mol^{-1} m^{3}s^{-1}, k_d = 10 s^{-1}, t = 1 s, D_M = 1. 10^{-9} m^2 s^{-1}, $D_{ML} = D_L$ = 5 10^-

^{10} m^2 s^{-1}. Dotted lines correspond to the effective metal profile given by the reaction layer thickness μ=3.33 10^{-9} m.

fig 2

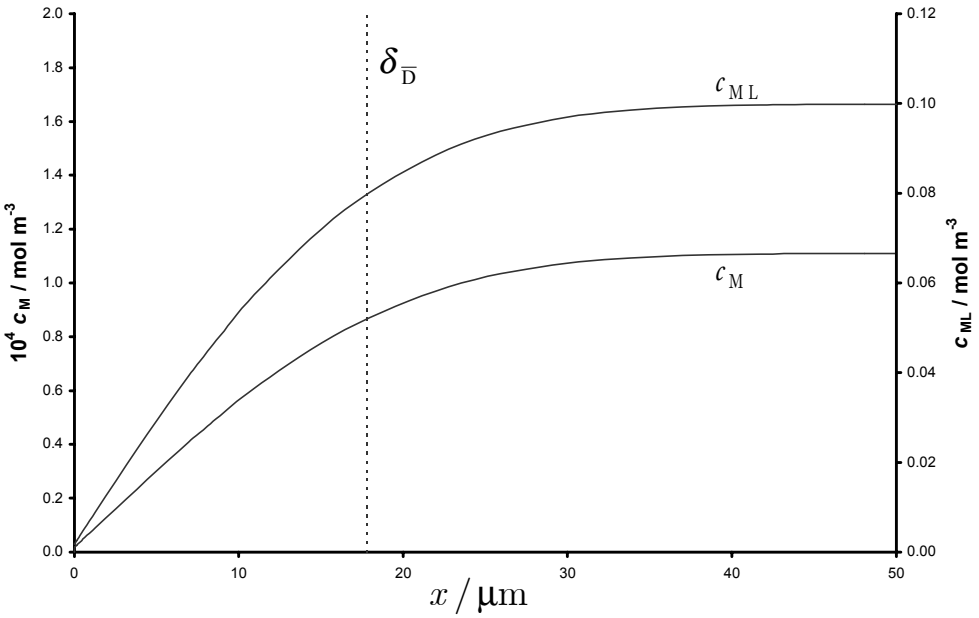

Fig 2: Concentration profiles of c_M and c_{ML} for a labile case. Parameters: k_a = 10^8 mol^{-1} m^{3}s^{-1}, k_d = 10^5 s^{-1}, K = 10^3 mol^{-1} m^3. Other parameters as in figure 1. The vertical dotted line indicates the thickness of the diffusion layer, $\delta_{\overline{D}} = \sqrt{\pi \overline{D} t}$.

fig. 3

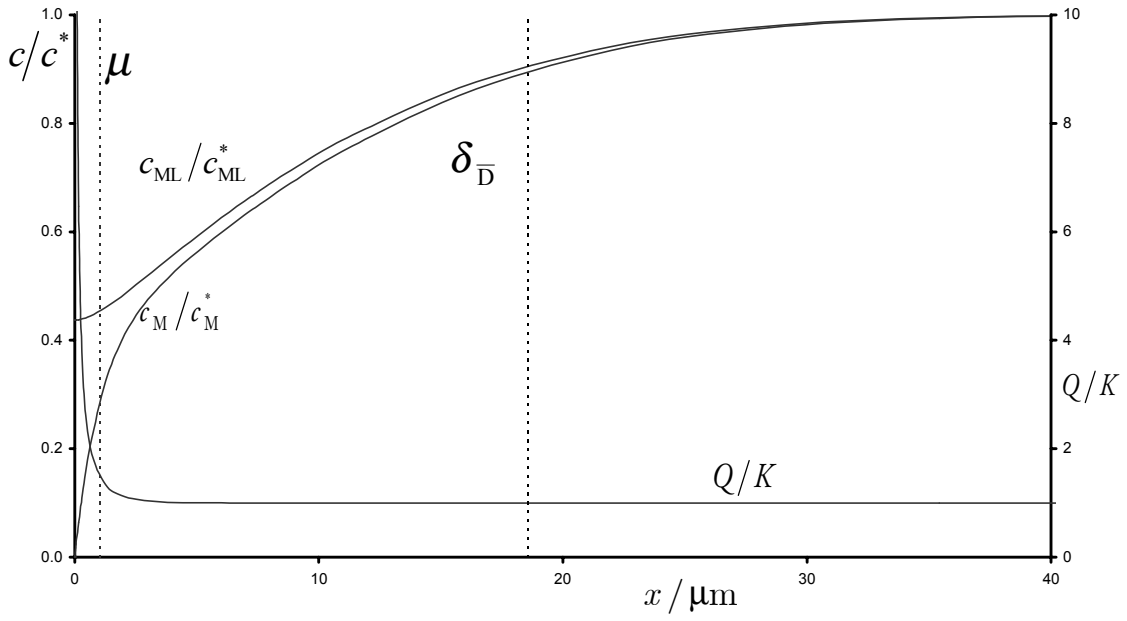

Published in Journal of Electroanalytical Chemistry 2002, vol 526, p 10-18
DOI: 10.1016/S0022-0728(02)00745-3
reprints also to galceran@quimica.udl.cat

Fig 3: Concentration profiles of $c_{\mathrm{M}}/c_{\mathrm{M}}^{*}$ and $c_{\mathrm{ML}}/c_{\mathrm{ML}}^{*}$ (referred to the left ordinate axis) and Q/K (referred to the right ordinate axis) for a partially-labile case. Parameters: k_a = 10^3 $\mathrm{mol^{-1}\ m^3 s^{-1}}$, k_d = 10 $\mathrm{s^{-1}}$. Other parameters as in figure 1. The vertical dotted lines indicate the end of the reaction layer at $x=\mu$ = 1.05 10^{-6} m and the end of the diffusion layer at $x=\delta_{\overline{\mathrm{D}}} = \sqrt{\pi\,\overline{\mathrm{D}}\,t}$ = 1.86 10^{-5} m

fig. 4

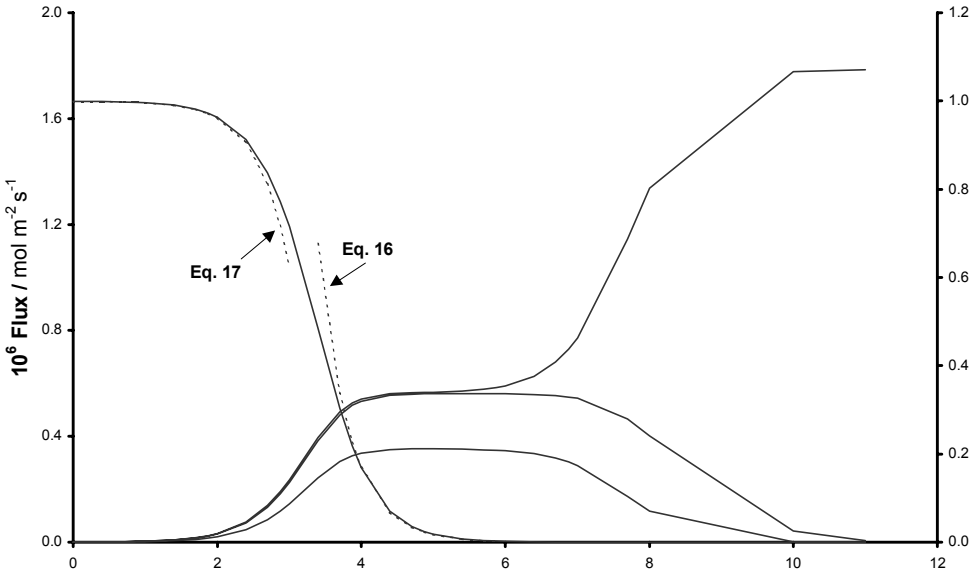

Fig 4: Plot of the metal flux at the electrode surface, $J_{\mathrm{M}}^{0} = D_{\mathrm{M}}\left(\dfrac{\partial c_{\mathrm{M}}}{\partial x}\right)_{x=0}$; the kinetic contribution, $J_{kin} = k_d\ c_{\mathrm{ML}}^{\phi}\ \mu$; the flux of complex arriving at the reaction layer, $J_{\mathrm{ML}}^{\mu} = D_{\mathrm{ML}}\left(\dfrac{\partial c_{\mathrm{ML}}}{\partial x}\right)_{x=\mu}$; and $c_{\mathrm{ML}}^{0}/c_{\mathrm{ML}}^{*}$ for increasing values of the dissociation kinetic constant. Other parameters as in fig. 1.

Published in Journal of Electroanalytical Chemistry 2002, vol 526, p 10-18
DOI: 10.1016/S0022-0728(02)00745-3
reprints also to galceran@quimica.udl.cat

fig. 5

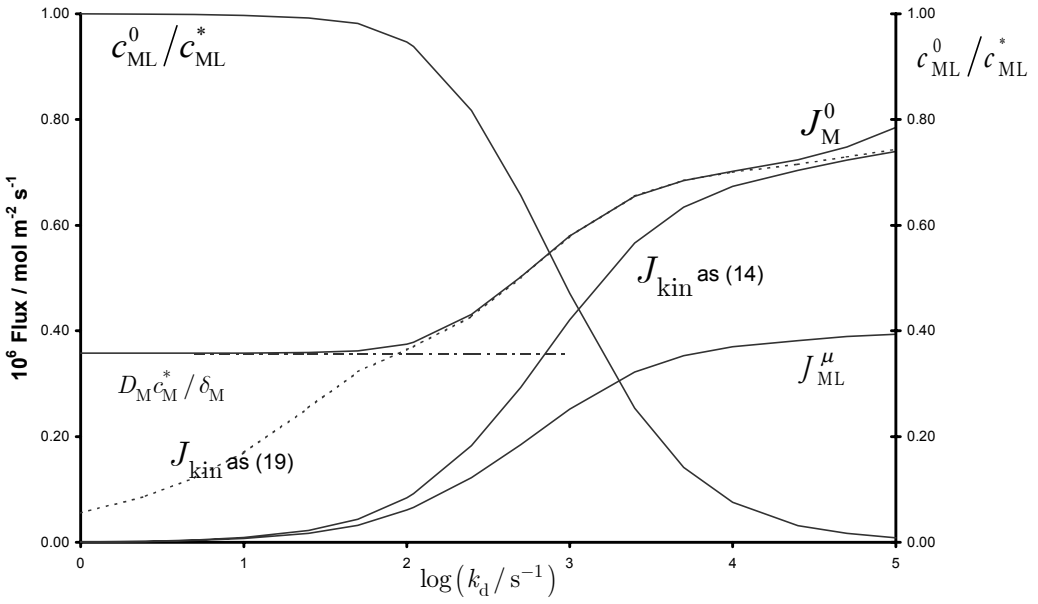

Fig. 5: Plot of the metal flux at the electrode surface, $J^0_{\mathrm{M}} = D_{\mathrm{M}}\left(\frac{\partial c_{\mathrm{M}}}{\partial x}\right)_{x=0}$; the kinetic contribution, J_{kin}, defined as (14), $J_{kin} = k_d\, c^{\phi}_{\mathrm{ML}}\, \mu$ (continuous line), or defined as (19), $J_{kin} = k_d\, c^{\phi}_{\mathrm{ML}} \mu^{\phi}$ (dotted line); the flux of complex incoming the reaction layer, $J^{\mu}_{\mathrm{ML}} = D_{\mathrm{ML}}\left(\frac{\partial c_{\mathrm{ML}}}{\partial x}\right)_{x=\mu}$; and $c^0_{\mathrm{ML}} / c^*_{\mathrm{ML}}$ *vs*. the dissociation kinetic constant for a non excess ligand system. Parameters are: $c^*_{\mathrm{T,L}}$ = 0.8 mol m^{-3}, $c^*_{\mathrm{T,M}}$ = 1 mol m^{-3}. Other parameters as in fig. 1. The inert flux value $D_{\mathrm{M}} c^*_{\mathrm{M}} / \delta_M$ is also plotted in dashed-dotted line.

fig. 6

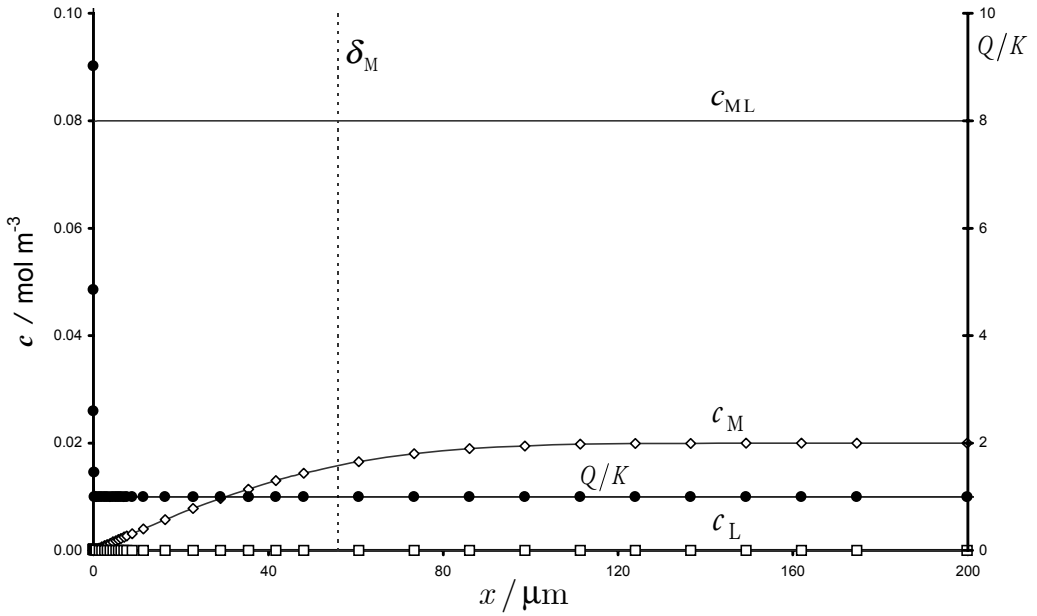

Fig 6: Concentration profiles for M (◊), L(□) and ML (*) corresponding to $k_d = 10\ s^{-1}$ in fig. 5. Concentrations are referred to the left *y*-axis, while *Q*/*K* (marker •) is referred to the right *y*-axis. The vertical dotted line indicates $\delta_M = \sqrt{\pi D_M t} = 5.61\ 10^{-5}$ m. Notice the explosion of the *Q*/*K* value close to the electrode surface.

fig. 7

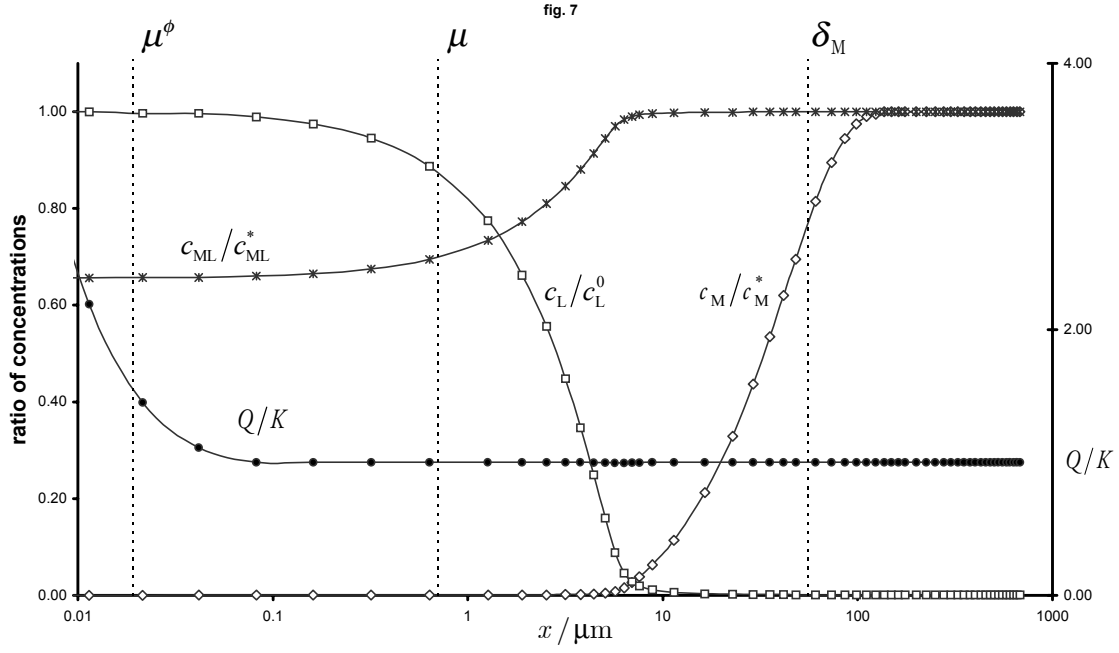

Fig 7: Normalized concentration profiles corresponding to k_d = 500 s^{-1} of fig. 5. The vertical dotted lines indicate μ^{ϕ} = 1.91 10^{-8} m, μ = 7.07 10^{-7} m and $\delta_M = \sqrt{\pi D_M t}$ = 5.61 10^{-5} m. Markers as in figure 6.

fig. 8

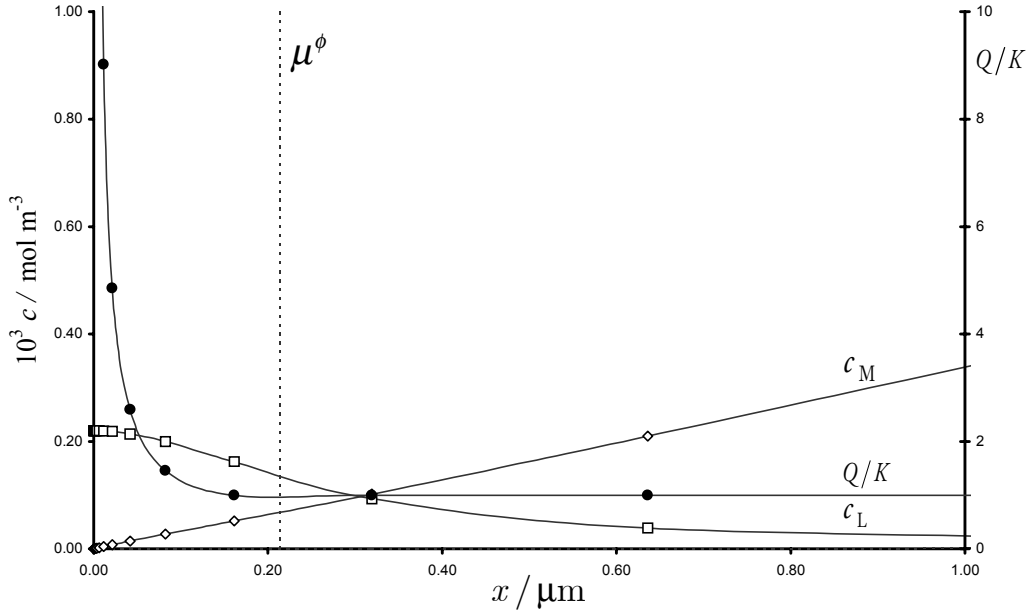

Fig. 8: Concentration profiles corresponding to k_d = 10 s^{-1} of fig. 5. Magnification of fig 6 up to distances from the electrode surface of the order of the reaction layer. The vertical dotted line indicates μ^{ϕ} = 2.13 10^{-7} m, while μ = 5.00 10^{-6} m is not seen in the figure.

Reference List

[1] J.Buffle, Complexation Reactions in Aquatic Systems. An Analytical Approach., Ellis Horwood Limited, Chichester, 1988.

[2] A.Tessier, J.Buffle and P.G.C.Campbell, in J. Buffle and R. DeVitre (Eds.), Chemical and Biological Regulation of Aquatic Systems, Lewis Publishers, Boca Raton, FL, 1994.

[3] Tessier, A. and Turner, D. R.Metal Speciation and Bioavailability in Aquatic Systems, John Wiley & Sons, Chichester. UK, 1995.

[4] D.R.Turner and M.Whitfield, J. Electroanal. Chem. 103 (1979) 61.

[5] H.G.DeJong and H.P.van Leeuwen, J. Electroanal. Chem. 234 (1987) 17.

[6] H.P. van Leeuwen, J.Buffle and R.Cleven, Pure Appl. Chem. 61 (1989) 255.

[7] J.Galceran, J.Puy, J.Salvador, J.Cecilia and H.P.van Leeuwen, J. Electroanal. Chem. 505 (2001) 85.

[8] T.M.Florence, Analyst 111 (1986) 489.

[9] R.Brdicka and K.Wiesner, Collect. Czech. Chem. Commun. 12 (1947) 39.

[10] R.Brdicka and K.Wiesner, Collect. Czech. Chem. Commun. 12 (1947) 138.

[11] J.Koutecky and R.Brdicka, Collect. Czech. Chem. Commun. 12 (1947) 337.

[12] J.Koutecky, Chem. Listy 47 (1953) 323.

[13] J.Koutecky, Collect. Czech. Chem. Commun. 18 (1953) 597.

[14] J.Heyrovsky, J.Kuta, Principles of Polarography, Academic Press, New York, 1966.

[15] J.Koutecky and J.Koryta, Electrochim. Acta 3 (1961) 318.

[16] J.Koryta, J.Dvorak and L.Kavan, Principles of Electrochemistry, Second ed. John Wiley, Chichester, 1993.

[17] E.Budewski, Compt. rend. Acad. Bulg. Sci. 8 (1955) 25.

[18] D.R.Crow, Polarography of Metal Complexes, Academic Press, London, 1969.

[19] W.Davison, J. Electroanal. Chem. 87 (1978) 395.

[20] H.P. van Leeuwen, J. Electroanal. Chem. 99 (1979) 93.

[21] H.P. van Leeuwen, Electroanal. 13 (2001) 826.

[22] J.Koutecky, Collect. Czech. Chem. Commun. 19 (1954) 857.

[23] H.G.DeJong, K.Holub and H.P.vanLeeuwen, J. Electroanal. Chem. 234 (1987) 1.

[24] J.Galceran, J.Cecilia, J.Salvador, J.Monne, M.Torrent, E.Companys, J.Puy, J.L.Garces and F.Mas, J. Electroanal. Chem. 472 (1999) 42.

[25] M.Lovric and I.Ruzic, J. Electroanal. Chem. 146 (1983) 253.

[26] K.B.Oldham, J. Electroanal. Chem. 313 (1991) 3.

[27] B.Vandenbossche, L.Bortels, J.Deconinck, S.Vandeputte and A.Hubin, J. Electroanal. Chem. 397 (1995) 35.

[28] T.J.R.Hughes, The Finite Element Method, Prentice Hall, Englewood Cliffs,N.J., 1987.

[29] J.Puy, J.Galceran, J.Salvador, J.Cecilia, J.M.Diazcruz, M.Esteban and F.Mas, J. Electroanal. Chem. 374 (1994) 223.

[30] J.Galceran, S.L.Taylor and P.N.Bartlett, J. Electroanal. Chem. 506 (2001) 65.

[31] W.H.Press, B.P.Flannery, S.A.Teukolsky and W.T.Vetterling, Numerical Recipes, Cambridge University Press, Cambridge, 1986.